

OMTN, Volume 33

Supplemental information

Targeting oncogenic *KRAS* in non-small cell lung cancer with EGFR aptamer-conjugated multifunctional RNA nanoparticles

Linlin Yang, Zhefeng Li, Daniel W. Binzel, Peixuan Guo, and Terence M. Williams

Table S1: Sequences used for construction of 3WJ pRNA nanoparticles.

ID	sequence
a: KRASG12C siRNA sense strand	5'-uuG ccA uGu GuA uGu GGG Guu GGa Gcu uGu GGc GuA Guu-3'
a': Scramble siRNA sense strand	5'-uuG ccA uGu GuA uGu GGG GGu cGA cGu ccA uuA ucu uuu-3'
b: EGFR aptamer strand	5'-ccc AcA uAc uuu Guu GAu ccG ccu uAG uAA cGu Gcu uuG AuG ucG Auu cGA cAG GAG Gc-3'
b': Scramble aptamer strand	5'-ccc AcA uAc uuu Guu GAu ccu ucG uAc cGG GuA GGU uGG cuu GcA cAu AGA AcG uGu ucA-3'
c: Strand without Alexa647	5'-GGA ucA Auc AuG GcA A-3'
c': strand for Alexa647 conjugation	5'-GGA ucA Auc AuG GcA A (C6-NH)(Alexa 647)-3'
d: KRASG12C siRNA antisense strand	5'-cuA cGc cAc AAG cuc cAA-3'
d': Scramble siRNA antisense strand	5'-AAG AuA AuG GAc Guc GAc c-3'

The lower letters indicated 2'-Fluoro modified nucleotides.

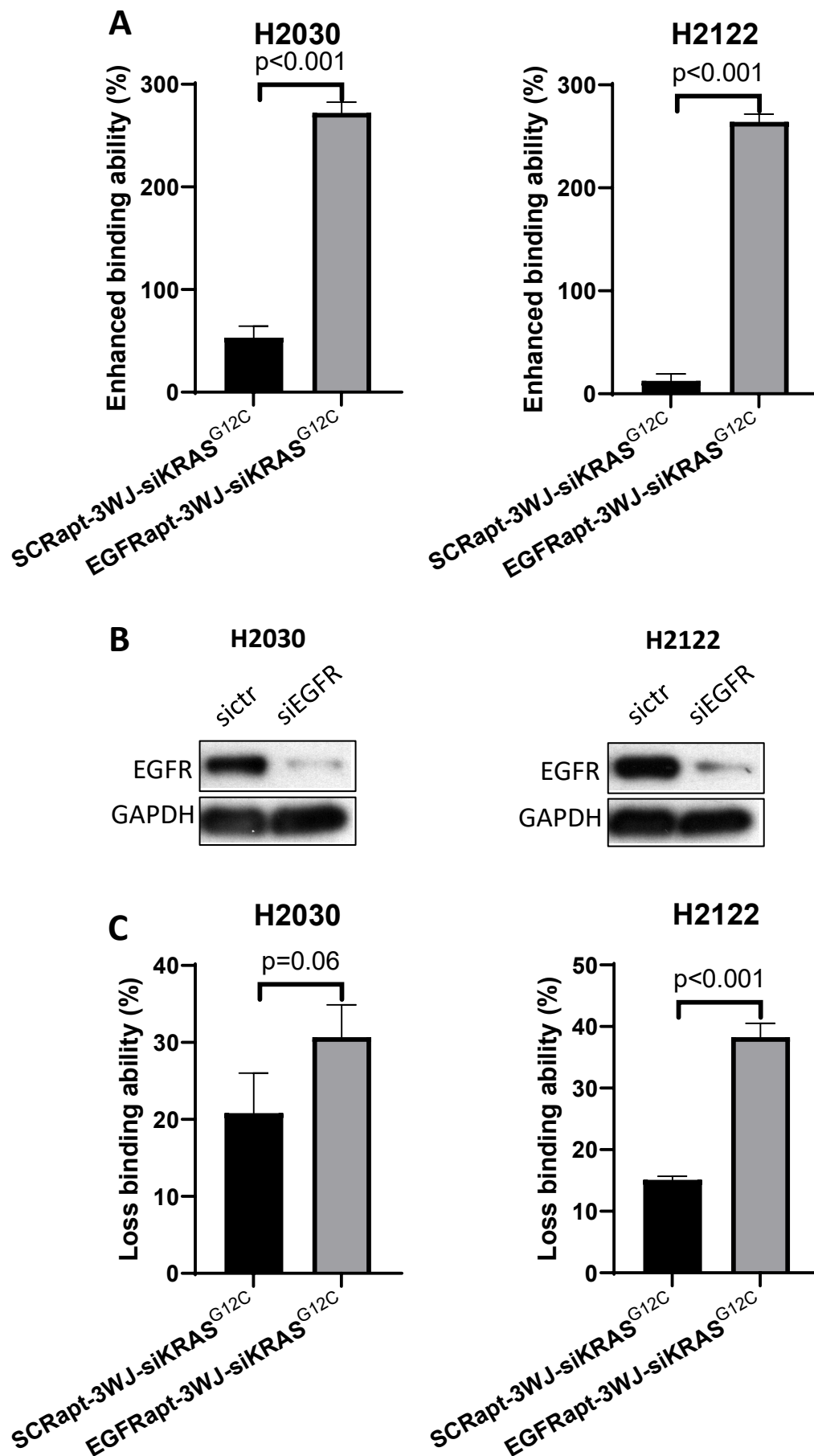


Figure S1. EGFR aptamer increased pRNA nanoparticle binding ability to NSCLC cells. A. Enhanced pRNA binding ability (%) by EGFR aptamer compared to non-aptamer pRNA nanoparticles (SCRapt). **B.** Immunoblotting confirms EGFR silencing by EGFR siRNA. **C.** Reduction in binding ability (%) of pRNA nanoparticles after EGFR silencing in NSCLC cells compared to non-targeting siRNA control cells (sictr).

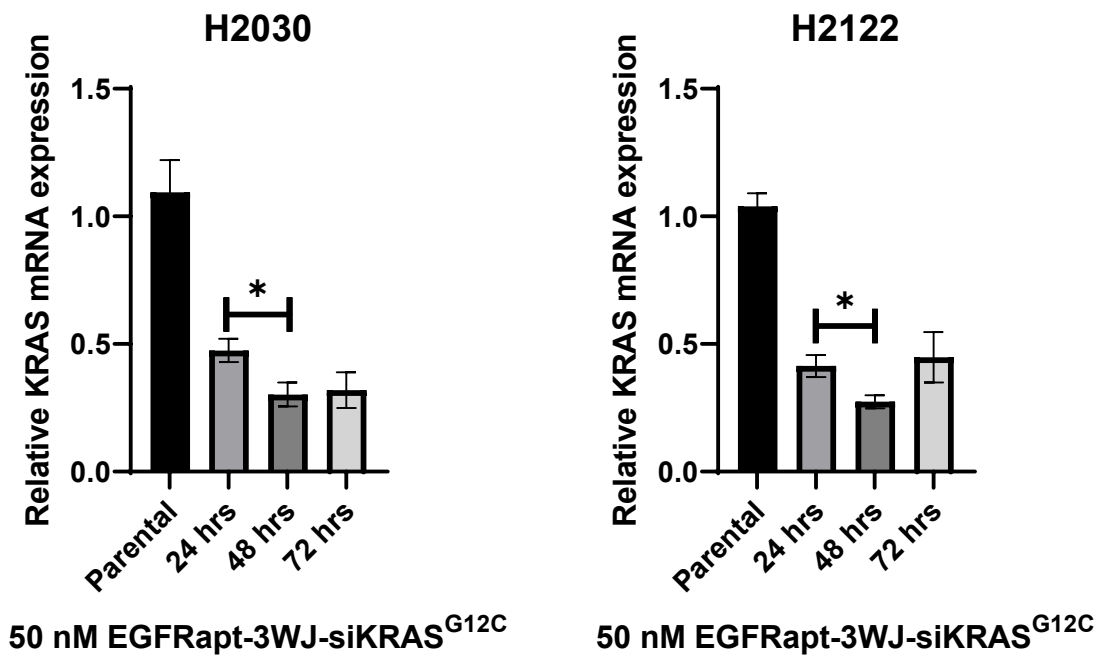
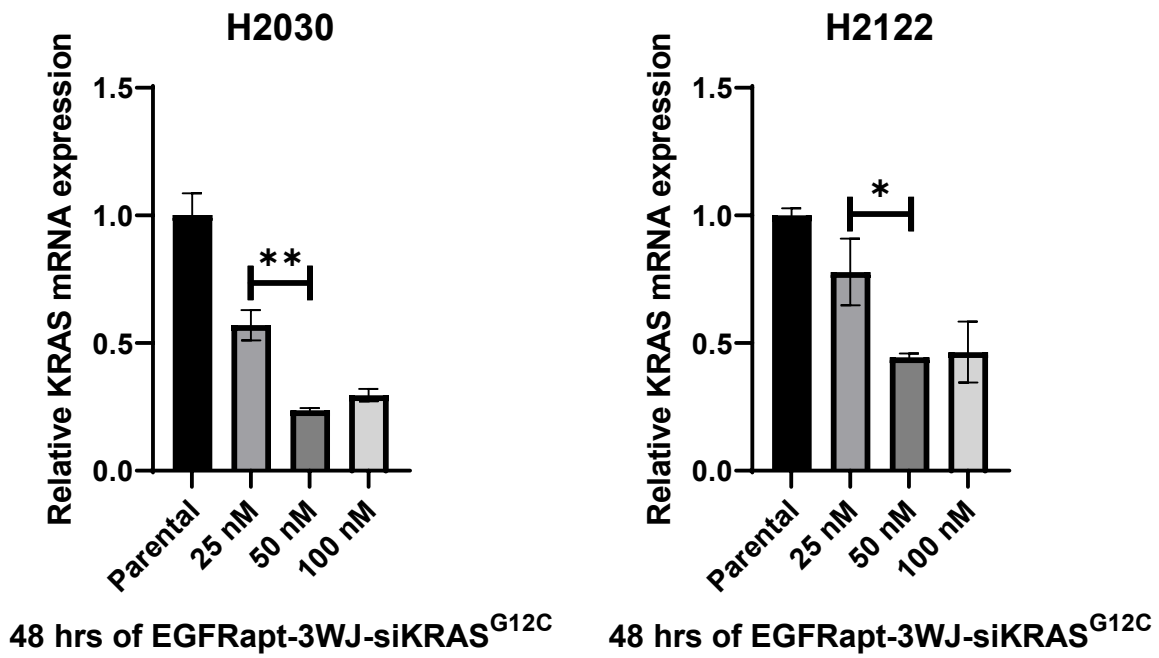


Figure S2. Dose and time course suppression of KRAS mRNA by EGFRapt-3WJ-siKRAS^{G12C} nanoparticles

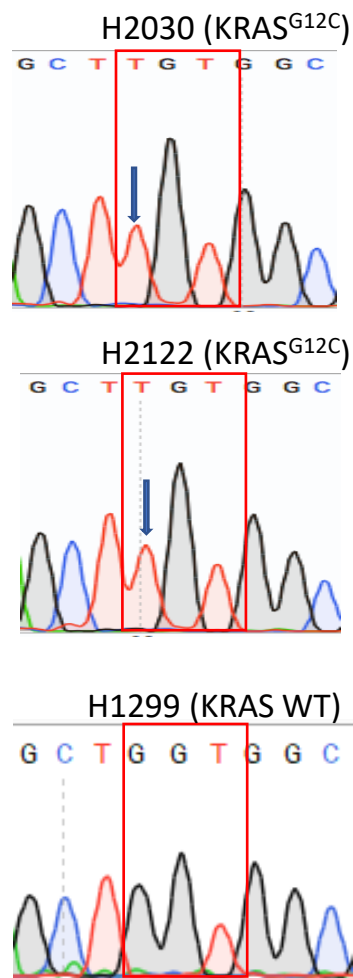


Figure S3. Sanger sequencing confirms the presence of KRAS^{G12C} mutations in H2030 and H2122 cells, and wild-type KRAS in H1299 cells.

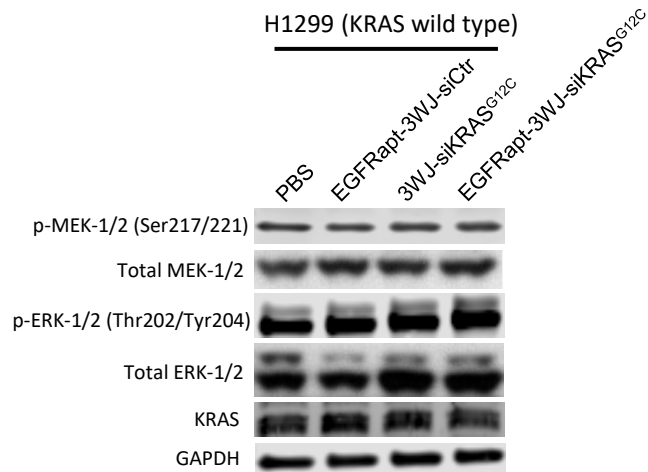
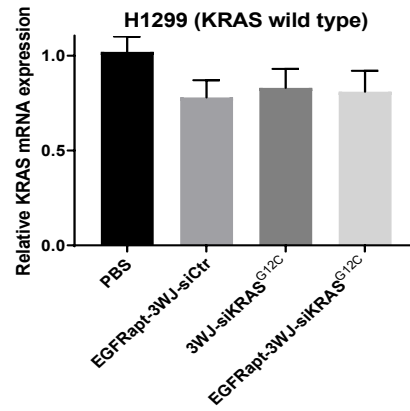


Figure S4. KRAS wild type NSCLC is not a target of EGFR_{apt}-3WJ-siKRAS^{G12C} pRNA nanoparticles

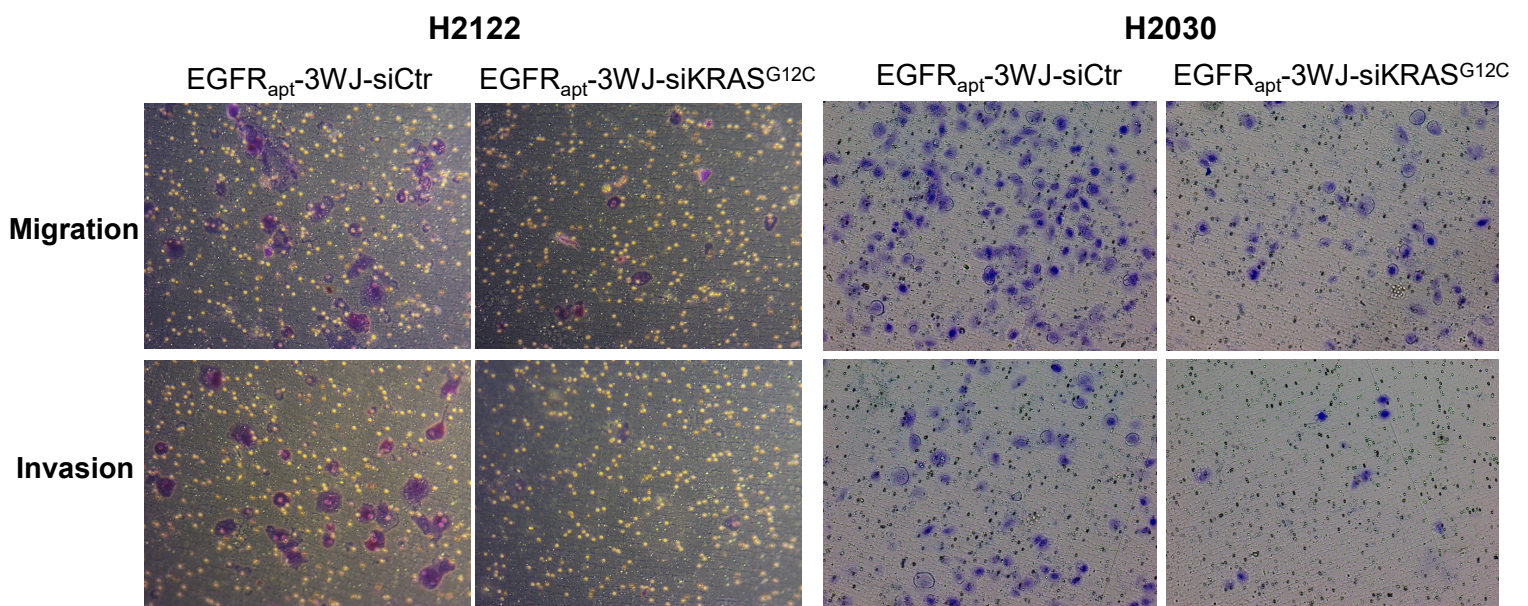


Figure S5. Representative pictures of migration and invasion assays in H2030 and H2122 cells.

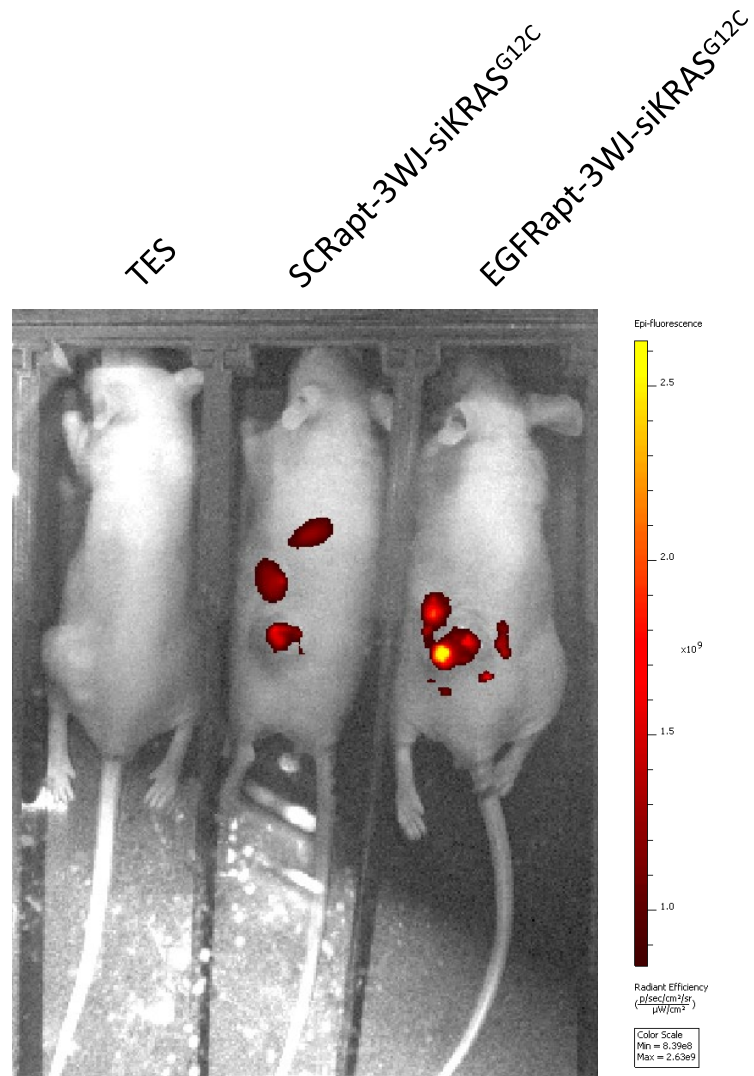


Figure S6. *In vivo* biodistribution of EGFRapt-3WJ-siKRAS^{G12C} and SCRapt-3WJ-siKRAS^{G12C} in H2122 tumor xenografts.